Construction and Myogenic Differentiation of 3D Myoblast Tissues Fabricated by Fibronectin-Gelatin Nanofilm Coating

Varvara Gribova[1], **Chen Yun Liu**[1], **Akihiro Nishiguchi**[1], **Michiya Matsusaki**[1], **Thomas Boudou**[2], **Catherine Picart**[2,*], and **Mitsuru Akashi**[1,*]

[1]Department of Applied Chemistry, Graduate School of Engineering, Osaka University, 2-1 Yamadaoka, Suita, Osaka 565-0871, Japan

[2]Grenoble Institute of Technology, CNRS UMR 5628, Laboratory of Materials and Physical Engineering, 3 parvis L. Néel, 38016 Grenoble, France

Abstract

In this study, we used a recently developed approach of coating the cells with fibronectin-gelatin nanofilms to build 3D skeletal muscle tissue models. We constructed the microtissues from C2C12 myoblasts and subsequently differentiated them to form muscle-like tissue. The thickness of the constructs could be successfully controlled by altering the number of seeded cells. We were able to build up to ~ 76 μm thick 3D constructs that formed multinucleated myotubes. We also found that Rho-kinase inhibitor Y27632 improved myotube formation in thick constructs. Our approach makes it possible to rapidly form 3D muscle tissues and is promising for the *in vitro* construction of physiologically relevant human skeletal muscle tissue models.

Keywords

Layer-by-layer; Tissue engineering; Extracellular matrix; Myogenesis

Introduction

Tissue engineering consists in combining stem cells and biomaterials to create tissues and organs *in vitro*, to improve the biological functions of damaged tissues or to replace them [1]. Development and regeneration of tissues is known to be strongly dependent on the cell microenvironment, especially on the signals that the cells receive from the extracellular matrix (ECM) and from neighbouring cells [2]. ECM induces stem cells to differentiate into mature tissue cells, provides structural support to the cells and determines tissue architecture and function [3].

The process of muscle formation requires that muscle precursor cells (myoblasts) proliferate, differentiate and fuse together to form multinucleated myotubes. Mature skeletal muscle has a complex three-dimensional (3D) organization of aligned muscle fibers surrounded by ECM [4] containing collagen, laminin and fibronectin [5,6,7].

---

[*]**Corresponding authors:** akashi@chem.eng.osaka-u.ac.jp (MA) catherine.picart@inp-grenoble.fr (CP).

One of the current challenges in muscle tissue engineering is to recreate functional 3D muscle tissues. Such engineered tissues may be used for the replacement of muscle after an injury, for drug screening, and for fundamental studies of muscle development and function. Many studies on skeletal muscle are carried out using 2D models. However, such models do not reproduce the complexity of 3D organization of the skeletal muscle *in vivo.* In addition, behavior of muscle progenitors, as well as differentiation, differ depending on whether they take place in 2D or 3D environment [8].

The most commonly used method for 3D muscle tissue construction consists in myoblast association to polymeric scaffolds. Some scaffolds made of synthetic polymers have been developed [9,10,11]. However, natural matrices such as collagen gels [12], matrigel [13,14] or fibrin gels [15] present advantages in view of their numerous interactions with muscle cells via specific receptors (such as integrins) and their capacity to bind specifically growth factors that are important for cell growth and differentiation [16]. Another method to create 3D muscle constructs is cell sheet-based tissue engineering. A thermoresponsive polymer, grafted on a cell culture substrate, allows confluent cells to be detached as a single cell sheet and to create scaffold-free 3D tissues by layering multiple cell sheets [17,18].

A new technology allowing fast and relatively simple construction of thick 3D tissues has recently been developed by our group. The method called "cell-accumulation technique" consists in coating the cells in a layer-by-layer manner [19] with fibronectin-gelatin (FN/G) films, before depositing on a substrate, onto which they spontaneously self-assemble to form tissue-like structures [20]. These ~10 nm thin (FN/G) coatings [21] provide the cells with an "artificial ECM" and enable cells to self-organize into 3D constructs. This was already applied successfully to construct ~ 35 μm thick human dermal fibroblasts 3D tissues, 8 layers of cells being formed after only one day of incubation [20], and to mesenchymal stem cells [22].

In this work, our aim was to build 3D muscle tissues using FN/G nanofilms and to characterize their morphology and differentiation state. Skeletal muscle ECM contains both FN and collagen (G being a collagen derivative) that interact with integrins and other adhesion receptors, thus playing important roles during skeletal muscle development and function [23,24]. We evaluated the morphological and histological characteristics of the 3D constructs obtained from C2C12 myoblasts, and analyzed the expression of myogenic markers in the microtissues cultured in myogenic differentiation medium.

Materials and Methods

Materials

C2C12 cells were purchased from ATCC. Dulbecco's modified Eagle medium (DMEM), 10% formalin solution (4% formaldehyde in water containing methanol), Tris (hydroxymethyl) aminomethane hydrochloride (Tris–HCl) and gelatin (G) were obtained from Wako Pure Chemical Industries (Osaka, Japan). Fetal bovine serum (FBS) was purchased from Biowest (Miami, USA). Horse serum was obtained from Gibco (New Zealand).The antibiotics were purchased from Nacalai Tesque (Kyoto, Japan). Bovine plasma fibronectin (FN) was purchased from Sigma–Aldrich (St. Louis, USA). Y27632 and

blebbistatin were obtained from Calbiochem. Primary antibodies: rabbit anti-myogenin (1:50) (Tebu-Bio, M225-sc576), mouse anti-troponin T (1:50) (Sigma, T6277) and rabbit anti-fibronectin (1:100) (Sigma, F3648). Secondary antibodies: goat anti-mouse Alexa-Fluor 488- and Alexa-Fluor 568-conjugated antibodies and goat anti-rabbit Alexa-Fluor 488-conjugated antibodies (Invitrogen, A11001, A11004 and A11008) were used at 1:1000. Phalloidin-TRITC was obtained from Sigma (P1951) and Hoechst 33342 from Invitrogen (H3570).

Cell culture

C2C12 cells (used at passages 5-15) were cultured in growth medium (GM) composed of Dulbecco's modified Eagle's medium (DMEM) medium supplemented with 10% fetal bovine serum containing 10 U/mL of penicillin G and 10 μg/mL of streptomycin. Cells were subcultured prior to reaching 60–70% confluence (approximately every 2 days). Cells were differentiated in a differentiation medium (DM) composed of DMEM supplemented with 2% horse serum and antibiotics.

Construction of microtissues

The microtissues were constructed by the cell-accumulation technique using the inserts with porous bottom to provide two-sided medium supply to thick multilayers (Fig 1A). Briefly, the cells were detached from culture dishes using trypsin 0,25% EDTA 0,02% and washed twice with the GM. After resuspending the cells in Tris-HCl buffer (Tris-HCl 50 mM pH 7,4), the cells were subsequently incubated for 1 min using a Microtube Rotater (MTR-103, AS ONE, Japan) with 0,04 mg/mL FN or G solutions in Tris-HCl buffer, then centrifuged at 200 g for 1 min, and the supernatant was gently removed by pipetting. After each FN or G deposition step the cells were rinsed in Tris-HCl buffer for 1 min using a Microtube Rotater, followed by centrifugation. When $(FN/G)_4FN$ nanofilms were formed, the cells were resuspended in GM and 300 μL of cell suspension was prepared at increasing cell number (10^5, 5 x 10^5, 10^6 and 2 x 10^6 cells per inset). For more clarity, the constructs will be named hereafter "1x", "5x", "10x" and "20x" (where x=10^5). The cells were deposited into 24-well inserts with a FN-precoated semipermeable membrane (Corning 3470, 0,4 μm pore size), which enables medium supply from the top and from the bottom (Fig 1B). FN pre-coating was depositing 100 μL of 0,04 mg/mL FN solution for 30 min at 37°C, then rinsing once with Tris-HCl buffer. 1 mL of GM was added in 24-well plate, respectively, outside the inserts. The cells were incubated for 2 h at 37°C, then another 1 mL of GM was added to 24-well plate to connect the media between the inside and the outside of the insert (Fig 1A). For the buildup of microtissues from non-coated (NC) cells considered here as a control, the cells were detached and seeded as described above, but the coating step was omitted. Hereafter, the constructs prepared from $(FN/G)_4FN$-coated cells will be named "FN/G-coated" (or "FN/G") constructs and those obtained from non-coated cells will be named "NC" constructs.

Histological analysis

The tissues were rinsed with phosphate buffered saline (PBS) solution, then incubated in 10% formaldehyde solution at room temperature for 30 min. The samples were then maintained in PBS solution before being mounted in paraffin-embedded blocks. These

paraffin-embedded blocks containing layered tissues were cut into 3–4 μm thick sections. The specimens were then stained with hematoxylin and eosin.

LIVE/DEAD viability assay inside the multilayered structures

The living and dead cells inside FN/G-coated and non-coated constructs were fluorescently labeled using a LIVE/DEAD viability assay kit accordingly to previously described procedure [25]. Briefly, calcein AM labels the living cells and ethidium homodimer-1 (EthD-1) labels the dead cells. Confocal laser scanning microscopy (CLSM) observations were performed using a FV10i (Olympus, Japan). For each 10x construct, the images were taken at three different levels, indicated as bottom: about 15 μm from the membrane, middle: 30μm and top: 45 μm.

Differentiation assays

Cells were differentiated in a differentiation medium (DM) composed of DMEM supplemented with 2% horse serum and antibiotics. Cells were then grown for 1 day in GM and then switched to DM. The medium was changed every 4 days. For differentiation assays in presence of Y27632 and blebbistatin, the cells were allowed to grow for 24 h in GM, then switched to DM supplemented with 5 μM Y2762 or blebbistatin. The fresh drugs were added every 2 days. Differentiation was characterized by the fusion index, which is the ratio of nuclei contained in myotubes to total number of nuclei [26].

Immunofluorescence analysis

Microtissues were first rinsed in PBS and fixed in 4% formaldehyde for 30 min at room temperature before being permeabilized in 0.5% Triton X-100 for 20 min. After rinsing with PBS, the samples were incubated for 3 h in 1% bovine serum albumin (BSA) in TRIS-buffered saline (TBS, 50 mM TRIS, 150 mM NaCl, 0.1% NaN_3, pH 7.4). Actin was labeled with phalloidin-TRITC (1:800) and cell nuclei were stained with 5 μg/ml Hoechst 33342 for 30 min. For immuno-staining, the tissues were incubated with the primary antibodies diluted in 1% BSA in TBS overnight at RT. The cells were washed three times with TBS and incubated for 3h at RT with the secondary antibodies. Fluorescent imaging of the obtained tissues was performed by CLSM with 10x and 60x objectives (FLUOVIEW FV10i, Olympus, Japan).

Statistics

Data are reported as means ± standard deviation. Box plot representations indicate the 25%, 50% and 75% of the values with lower and upper boundaries being 10 and 90%. Experiments were reproduced in duplicate or triplicate. Statistical comparisons were performed using SigmaPlot Version 11.0 software and based on an analysis of variance (ANOVA) followed by an appropriate pairwise comparison, or on Student's test. ($P < 0.05$) was considered significant. Statistically different values are reported on the figures.

Results

Construction of microtissues from C2C12 myoblasts

The 3D microtissues were formed by coating the surface of C2C12 myoblasts with (FN/G)$_4$FN nanofilms and then seeding an increasing cell number (from 1x to 20x, where x=10^5) in 24-well porous inserts (Fig 1A). Fibronectin labeling after 24h of culture in GM revealed fibrillar network surrounding the cells in FN/G-coated 10x constructs (Fig 1B). FN coating was also previously visualized on single coated cells [27].

Histological characterization of microtissues and thickness quantification

Next, we studied the influence of the number of seeded cells on tissue formation and thickness. We performed analysis of the histological cross-sections in Z after 24h in GM (Fig 2A) and quantified tissue thickness (Fig 2B). As expected, the thickness increased with the initial cell number. The thickness of 1x, 5x and 10x tissues after 24h of culture in GM was 8±3 μm, 29.2±1.2 μm and 63.4±7 μm for FN/G-coated constructs as compared to 8.3±1.4 μm, 22.2±2 μm and 41.9±6 μm for NC constructs (Fig 2B). The 20x constructs were discarded from the subsequent studies because they formed cell aggregates and detached (Fig 2C).

As showed our cell viability assays (Fig 2D and Table 1), there was no big difference of cell viability between FN/G-coated and non-coated constructs. However, live/dead cell ratio was decreased in the lower side of the constructs compared to the upper side (Fig S1A). As it was also shown that only very few cells proliferated in thick FN/G-coated constructs (Fig S1B), higher thickness of FN/G-constructs is probably due to a higher adhesion between the cells provided by FN/G-coating rather than by a higher cell proliferation.

Myogenic differentiation of microtissues is impaired in thick constructs

C2C12 myoblasts are a well-known model for the *in vitro* study of myogenic differentiation due to their ability to reproduce processes that take place during *in vivo* differentiation of skeletal muscle progenitors [28,29]. For the construction of functional 3D skeletal muscle tissue models *in vitro*, the formation of myotubes by fusion of myoblasts is a crucial step. We induced the differentiation of 10x FN/G-coated and non-coated constructs by culturing them in differentiation medium (DM), then stained them for myogenin, which is an early marker of myogenic differentiation, and troponin T, which is a part of troponin-tropomyosin complex involved in muscle contraction.

The analysis of expression of myogenin (Fig 3A) showed no big difference of its expression at Day 2 of differentiation between FN/G-coated and non-coated constructs. However, the expression was very low for both 10x constructs, with only few myogenin-positive nuclei (Fig 3B). Nevertheless, non-coated 10x constructs were still able to undergo myogenic differentiation, as troponin T positive myotubes were visible in non-coated 10x constructs after 4 days in DM (Fig 3C). FN/G-coated 10x constructs presented some troponin T staining, but almost no myotubes could be observed.

Rho-kinase inhibition improves myogenic differentiation in thick constructs

In addition to lower differentiation, partial detachment at the periphery of thick FN/G-coated constructs cultured in DM could be observed (Fig 4A). We hypothetized that this detachment could be due to high cell contractility in thick constructs. To decrease the cellular tension, we selected two contractility inhibitors: blebbistatin, which inhibits myosin II [30] and Y27632 (Y27), a Rho kinase (ROCK) inhibitor [31], thus preventing the contraction. Blebbistatin was found to prevent detachment but also to negatively affect myogenic differentiation (data not shown) and was discarded from the study. In contrast, Y27 not only prevented cell detachment (Fig 4A), but, surprisingly, improved myogenic differentiation (Fig 4B), increasing the fusion index from $2.04 \pm 1.40\%$ to $9.93 \pm 3.45\%$ (Fig 4C). Also, expression of a late myogenic marker skeletal myosin increased in FN/G-coated and Y27-treated constructs compared to FN/G-coated non-treated (Fig S2).

In addition, Y27-treated 10x FN/G-coated constructs appeared to be about two times thicker than non-coated: 76.5 ± 18.0 and 35.0 ± 5.0 μm, respectively, and thicker that FN/G-coated construct non treated with Y27 (55.1 ± 9.8) (Fig 4D and E).

Thus, treatment with the ROCK inhibitor Y27 allowed to increase the thickness of FN/G-coated constructs up to 76 μm and improve their differentiation. The analysis of thickness also revealed an advantage of the FN/G coating for the formation of thicker 3D skeletal muscle tissue models, compared to non-coated constructs.

Discussion

One of the current challenges in muscle tissue engineering is to construct physiologically relevant 3D muscle tissues. In this work, we built 3D skeletal muscle tissues by a simple and rapid self-assembly technique using FN/G pre-coated C2C12 myoblasts. We defined the conditions for optimal 3D muscle tissue formation by this technique, i.e. a tissue that does not detach and can be maintained until myotube formation and expression of a differentiation marker, troponin T. We studied the influence of the number of cells initially seeded and found that tissues could be formed in a certain range (up to 10^6 cells), whereas a too high number of cells (2×10^6) led to heterogeneous and non-cohesive tissues. This phenomenon of aggregation might be related to lack of nutrient supply inside such thick constructs and may be overcome by creating a vascular network within the constructs. Indeed, an important challenge in tissue engineering field consists in vascularizing engineered 3D tissues, since blood supply is necessary to bring nutritive elements and oxygen to the cells in thick constructs [32]. The cell-accumulation technique may allow such vascularization by including endothelial cells in the architecture, as was recently shown for a fibroblast/endothelial cell tissue prepared by alternate deposits of coated cells in a layer-by-layer manner [20,22].

As expected, the thickness of microtissues increased with increasing cell number. These data are in agreement with the previous study [20]. The ROCK inhibitor was found to help 3D tissue formation by preventing tissue detachment from the underlying substrate. These results confirmed the important role of cell contractility in the formation and maintenance of differentiated 3D muscle tissues.

The effect of Y27 on myotube formation may be related to the importance of ROCK in myoblast differentiation. Indeed, it is known that ROCK inhibition occurs naturally during myogenic differentiation [33,34], so using Y27 may help to mimic a physiological situation. To our knowledge, in 3D, the effect of Y27 on myoblast differentiation has never been described so far.

Stress fiber formation is closely related to the stiffness of the cell environment [35,36], and it is now acknowledged that mechanical properties of the 2D substrate can affect muscle cell adhesion, spreading, proliferation and differentiation [37,38,39,40]. In 3D myogenic differentiation was studied using alginate gels of various degradability [8], fibrin gels [15] or polymer scaffold composed of poly-(L-lactic acid)/poly(lactic-glycolic) acid [41]. However, the results vary depending on the type of the scaffold, and different steps of myogenic differentiation in 3D require further investigation using physiological models of muscle tissues. In this context, muscle constructs fabricated by cell-accumulation method can become a useful model system to study myogenic differentiation in 3D.

The cell-accumulation technique opens new perspectives for creating more complex and more physiological tissue models. Because *in vivo* muscle environment can vary in matrix composition depending on muscle type, location and individual variability, cell coating may be adjusted to better mimic specific muscle ECM. Different cell types, such as endothelial cells for vascularization or fibroblasts for ECM production may be co-cultured with myoblasts using derivatives of the cell-accumulation method, e.g. sandwich culture. Finally, the technique does not require complex cell manipulation and may be used by a wide range of researchers.

Supporting Information

Refer to Web version on PubMed Central for supplementary material.

Acknowledgements

References

[1]. Lutolf MP, Hubbell JA. Synthetic biomaterials as instructive extracellular microenvironments for morphogenesis in tissue engineering. Nat Biotechnol. 2005; 23:47–55. [PubMed: 15637621]

[2]. Hynes RO. The extracellular matrix: not just pretty fibrils. Science. 2009; 326:1216–1219. [PubMed: 19965464]

[3]. Reilly GC, Engler AJ. Intrinsic extracellular matrix properties regulate stem cell differentiation. J Biomech. 2010; 43:55–62. [PubMed: 19800626]

[4]. Light N, Champion AE. Characterization of muscle epimysium, perimysium and endomysium collagens. Biochem J. 1984; 219:1017–1026. [PubMed: 6743238]

[5]. Gillies AR, Lieber RL. Structure and function of the skeletal muscle extracellular matrix. Muscle Nerve. 2011; 44:318–331. [PubMed: 21949456]

[6]. Thorsteinsdottir S, Deries M, Cachaco AS, Bajanca F. The extracellular matrix dimension of skeletal muscle development. Dev Biol. 2011; 354:191–207. [PubMed: 21420400]

[7]. Hinds S, Bian W, Dennis RG, Bursac N. The role of extracellular matrix composition in structure and function of bioengineered skeletal muscle. Biomaterials. 2011; 32:3575–3583. [PubMed: 21324402]

[8]. Boontheekul T, Hill EE, Kong HJ, Mooney DJ. Regulating myoblast phenotype through controlled gel stiffness and degradation. Tissue Eng. 2007; 13:1431–1442. [PubMed: 17561804]

[9]. Shah R, Sinanan AC, Knowles JC, Hunt NP, Lewis MP. Craniofacial muscle engineering using a 3-dimensional phosphate glass fibre construct. Biomaterials. 2005; 26:1497–1505. [PubMed: 15522751]

[10]. Williamson MR, Adams EF, Coombes AG. Gravity spun polycaprolactone fibres for soft tissue engineering: interaction with fibroblasts and myoblasts in cell culture. Biomaterials. 2006; 27:1019–1026. [PubMed: 16054685]

[11]. Levenberg S, Rouwkema J, Macdonald M, Garfein ES, Kohane DS, Darland DC, Marini R, van Blitterswijk CA, Mulligan RC, D'Amore PA, Langer R. Engineering vascularized skeletal muscle tissue. Nat Biotechnol. 2005; 23:879–884. [PubMed: 15965465]

[12]. Bian W, Bursac N. Engineered skeletal muscle tissue networks with controllable architecture. Biomaterials. 2009; 30:1401–1412. [PubMed: 19070360]

[13]. Bian W, Juhas M, Pfeiler TW, Bursac N. Local tissue geometry determines contractile force generation of engineered muscle networks. Tissue Eng Part A. 2012; 18:957–967. [PubMed: 22115339]

[14]. Vandenburgh H, Shansky J, Benesch-Lee F, Barbata V, Reid J, Thorrez L, Valentini R, Crawford G. Drug-screening platform based on the contractility of tissue-engineered muscle. Muscle Nerve. 2008; 37:438–447. [PubMed: 18236465]

[15]. Chiron S, Tomczak C, Duperray A, Laine J, Bonne G, Eder A, Hansen A, Eschenhagen T, Verdier C, Coirault C. Complex interactions between human myoblasts and the surrounding 3D fibrin-based matrix. PLoS One. 2012; 7:e36173. [PubMed: 22558372]

[16]. Janmey PA, Winer JP, Weisel JW. Fibrin gels and their clinical and bioengineering applications. J R Soc Interface. 2009; 6:1–10. [PubMed: 18801715]

[17]. Yamada N, Okano T, Sakai H, Karikusa F, Sawasaki Y, Sakurai Y. Thermo-responsive polymeric surfaces; control of attachment and detachment of cultured cells. Makromol Chem Rapid Comm. 1990; 11:571–576.

[18]. Akiyama Y, Kikuchi A, Yamato M, Okano T. Ultrathin poly(N-isopropylacrylamide) grafted layer on polystyrene surfaces for cell adhesion/detachment control. Langmuir. 2004; 20:5506–5511. [PubMed: 15986693]

[19]. Decher G. Fuzzy Nanoassemblies: Toward Layered Polymeric Multicomposites. Science. 1997; 277:1232–1237.

[20]. Nishiguchi A, Yoshida H, Matsusaki M, Akashi M. Rapid construction of three-dimensional multilayered tissues with endothelial tube networks by the cell-accumulation technique. Adv Mater. 2011; 23:3506–3510. [PubMed: 21728193]

[21]. Matsusaki M, Kadowaki K, Nakahara Y, Akashi M. Fabrication of Cellular Multilayers with Nanometer-Sized Extracellular Matrix Films. Angew Chem. 2007; 46:4689–4692. [PubMed: 17503408]

[22]. Nishiguchi A, Matsusaki M, Asano Y, Shimoda H, Akashi M. Effects of angiogenic factors and 3D-microenvironments on vascularization within sandwich cultures. Biomaterials. 2014; 35:4739–4748. [PubMed: 24655783]

[23]. Perkins AD, Ellis SJ, Asghari P, Shamsian A, Moore ED, Tanentzapf G. Integrin-mediated adhesion maintains sarcomeric integrity. Dev Biol. 2010; 338:15–27. [PubMed: 19879257]

[24]. Mayer U. Integrins: redundant or important players in skeletal muscle? J Biol Chem. 2003; 278:14587–14590. [PubMed: 12556453]

[25]. Chetprayoon P, Kadowaki K, Matsusaki M, Akashi M. Survival and structural evaluations of three-dimensional tissues fabricated by the hierarchical cell manipulation technique. Acta Biomater. 2013; 9:4698–4706. [PubMed: 22917803]

[26]. Charrasse S, Comunale F, Grumbach Y, Poulat F, Blangy A, Gauthier-Rouviere C. RhoA GTPase regulates M-cadherin activity and myoblast fusion. Mol Biol Cell. 2006; 17:749–759. [PubMed: 16291866]

[27]. Matsusaki M, Kadowaki K, Adachi E, Sakura T, Yokoyama U, Ishikawa Y, Akashi M. Morphological and histological evaluations of 3D-layered blood vessel constructs prepared by hierarchical cell manipulation. J Biomater Sci Polym Ed. 2012; 23:63–79. [PubMed: 21176392]

[28]. Andres V, Walsh K. Myogenin expression, cell cycle withdrawal, and phenotypic differentiation are temporally separable events that precede cell fusion upon myogenesis. J Cell Biol. 1996; 132:657–666. [PubMed: 8647896]

[29]. Bach AD, Beier JP, Stern-Staeter J, Horch RE. Skeletal muscle tissue engineering. J Cell Mol Med. 2004; 8:413–422. [PubMed: 15601570]

[30]. Kovacs M, Toth J, Hetenyi C, Malnasi-Csizmadia A, Sellers JR. Mechanism of blebbistatin inhibition of myosin II. J Biol Chem. 2004; 279:35557–35563. [PubMed: 15205456]

[31]. Uehata M, Ishizaki T, Satoh H, Ono T, Kawahara T, Morishita T, Tamakawa H, Yamagami K, Inui J, Maekawa M, Narumiya S. Calcium sensitization of smooth muscle mediated by a Rho-associated protein kinase in hypertension. Nature. 1997; 389:990–994. [PubMed: 9353125]

[32]. Koning M, Harmsen MC, van Luyn MJ, Werker PM. Current opportunities and challenges in skeletal muscle tissue engineering. J Tissue Eng Regen Med. 2009; 3:407–415. [PubMed: 19575392]

[33]. Nishiyama T, Kii I, Kudo A. Inactivation of Rho/ROCK signaling is crucial for the nuclear accumulation of FKHR and myoblast fusion. J Biol Chem. 2004; 279:47311–47319. [PubMed: 15322110]

[34]. Castellani L, Salvati E, Alema S, Falcone G. Fine regulation of RhoA and Rock is required for skeletal muscle differentiation. J Biol Chem. 2006; 281:15249–15257. [PubMed: 16574652]

[35]. Walcott S, Sun SX. A mechanical model of actin stress fiber formation and substrate elasticity sensing in adherent cells. Proc Natl Acad Sci U S A. 2010; 107:7757–7762. [PubMed: 20385838]

[36]. Yeung T, Georges PC, Flanagan LA, Marg B, Ortiz M, Funaki M, Zahir N, Ming W, Weaver V, Janmey PA. Effects of substrate stiffness on cell morphology, cytoskeletal structure, and adhesion. Cell Motil Cytoskeleton. 2005; 60:24–34. [PubMed: 15573414]

[37]. Engler AJ, Griffin MA, Sen S, Bonnemann CG, Sweeney HL, Discher DE. Myotubes differentiate optimally on substrates with tissue-like stiffness: pathological implications for soft or stiff microenvironments. J Cell Biol. 2004; 166:877–887. [PubMed: 15364962]

[38]. Gribova V, Gauthier-Rouvière C, Albigès-Rizo C, Auzely-Velty R, Picart C. Effect of RGD functionalization and stiffness modulation of polyelectrolyte multilayer films on muscle cell differentiation. Acta Biomater. 2013; 9:6468–6480. [PubMed: 23261924]

[39]. Ren K, Crouzier T, Roy C, Picart C. Polyelectrolyte multilayer films of controlled stiffness modulate myoblast cells differentiation. Adv Funct Mater. 2008; 18:1378–1389. [PubMed: 18841249]

[40]. Gilbert PM, Havenstrite KL, Magnusson KE, Sacco A, Leonardi NA, Kraft P, Nguyen NK, Thrun S, Lutolf MP, Blau HM. Substrate elasticity regulates skeletal muscle stem cell self-renewal in culture. Science. 2010; 329:1078–1081. [PubMed: 20647425]

[41]. Levy-Mishali M, Zoldan J, Levenberg S. Effect of scaffold stiffness on myoblast differentiation. Tissue Eng Part A. 2009; 15:935–944. [PubMed: 18821844]
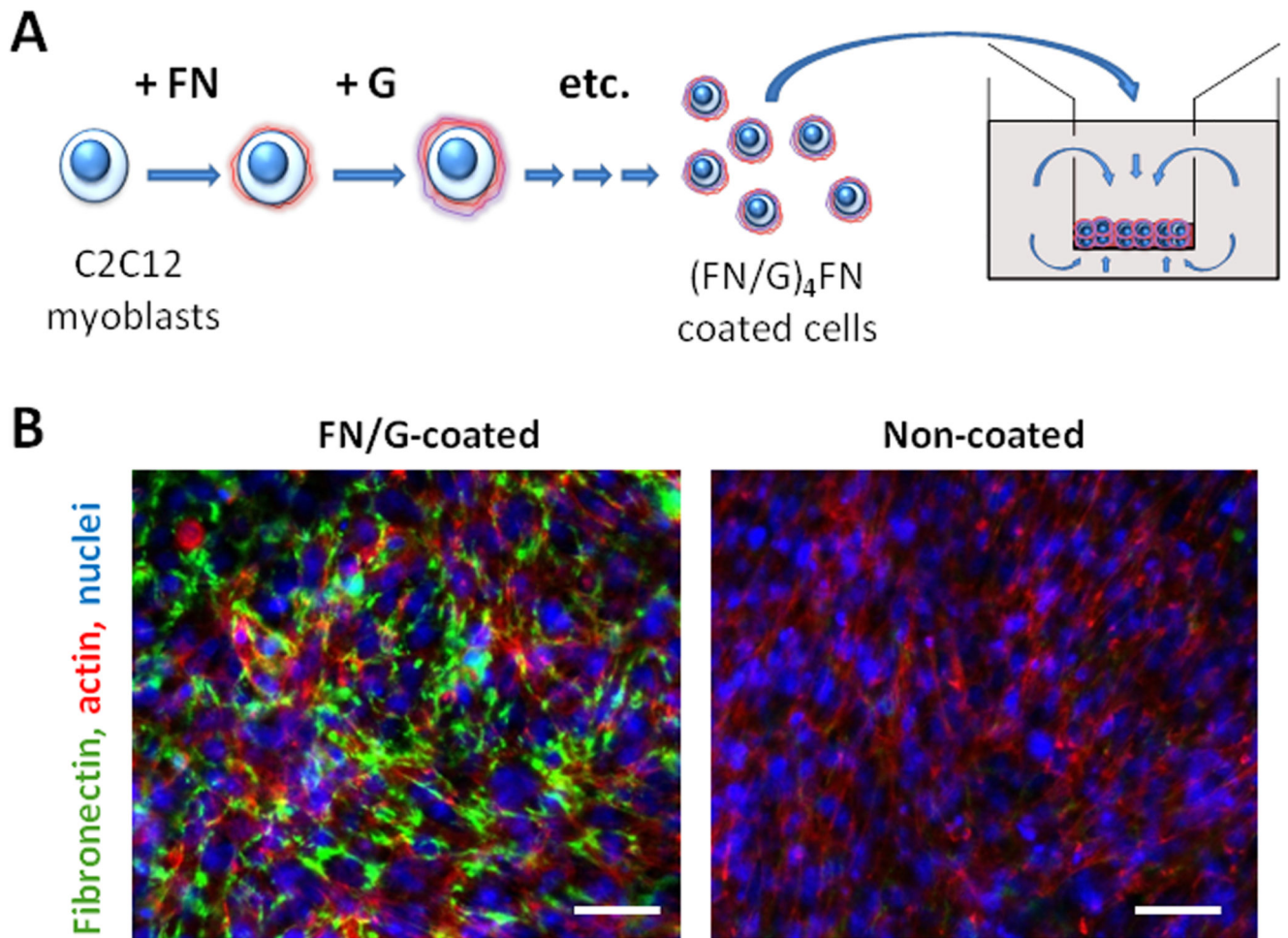
Fig 1. Construction of skeletal muscle microtissues by cell-accumulation technique.
(A) Scheme of the cell coating by $(FN/G)_4FN$ nanofilms and self-assembly of coated cells in multilayered tissues, once introduced in 24-well inserts that enables medium supply by both sides (top and bottom of the cellular tissue). (B) Visualization of FN matrix: confocal microscopy images of fibronectin (green), actin (red) and nuclei (blue) staining of FN/G-coated and non-coated 10x constructs after 24 h of culture in GM. Scale bar: 50 μm.
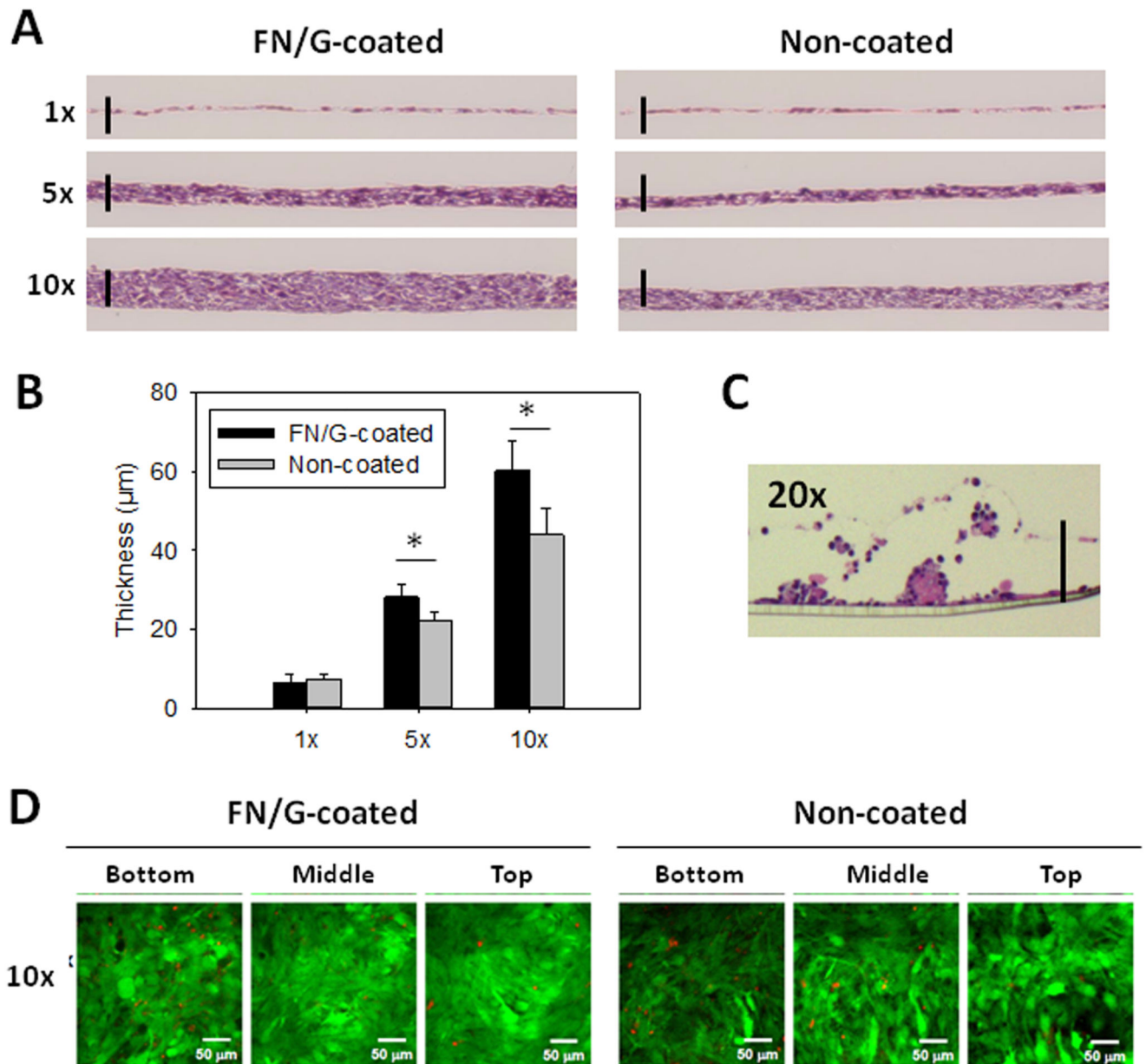
Fig 2. Histological characterization and thickness quantification of skeletal muscle microtissues.
(A) Histological analysis of FN/G-coated and non-coated constructs: phase contrast microscopy observations of hematoxylin-eosin stained cross-sections in Z of 1x, 5x and 10x constructs after 24 h of culture in GM. Scale bar: 50 μm. (B) Quantification of the thickness after 24 h of culture in GM (n=3, *p<0.05). (C) Hematoxylin-eosin stained cross-sections of 20x construct after 24 h of culture in GM. (D) Live (green)/Dead (red) staining. Bottom: about 15 μm from the membrane, middle: 30μm and top: 45 μm. Scale bar: 50 μm.
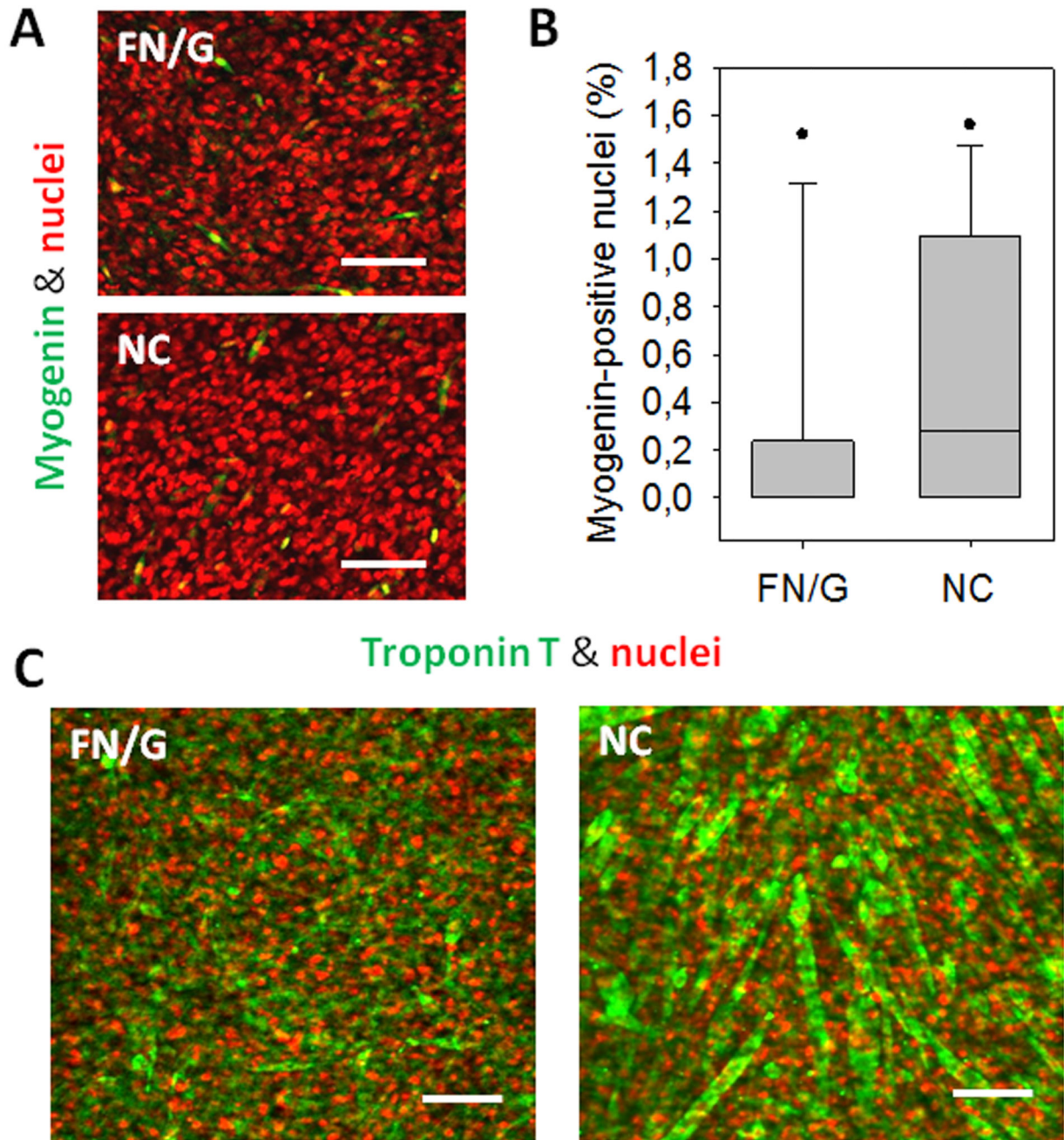
Fig 3. Myogenic differentiation of skeletal muscle microtissues.
(A) Nuclei (red) and myogenin (green) labelling of 10x constructs at Day 2 of differentiation. Scale bar: 50 μm. (B) Quantification of myogenin-positive nuclei in 10x constructs at Day 2 of differentiation (n=3). (C) Confocal microscopy images of troponin T (green) and nuclei (red) staining of 10x constructs after 4 days in differentiation medium. Scale bar: 100 μm.
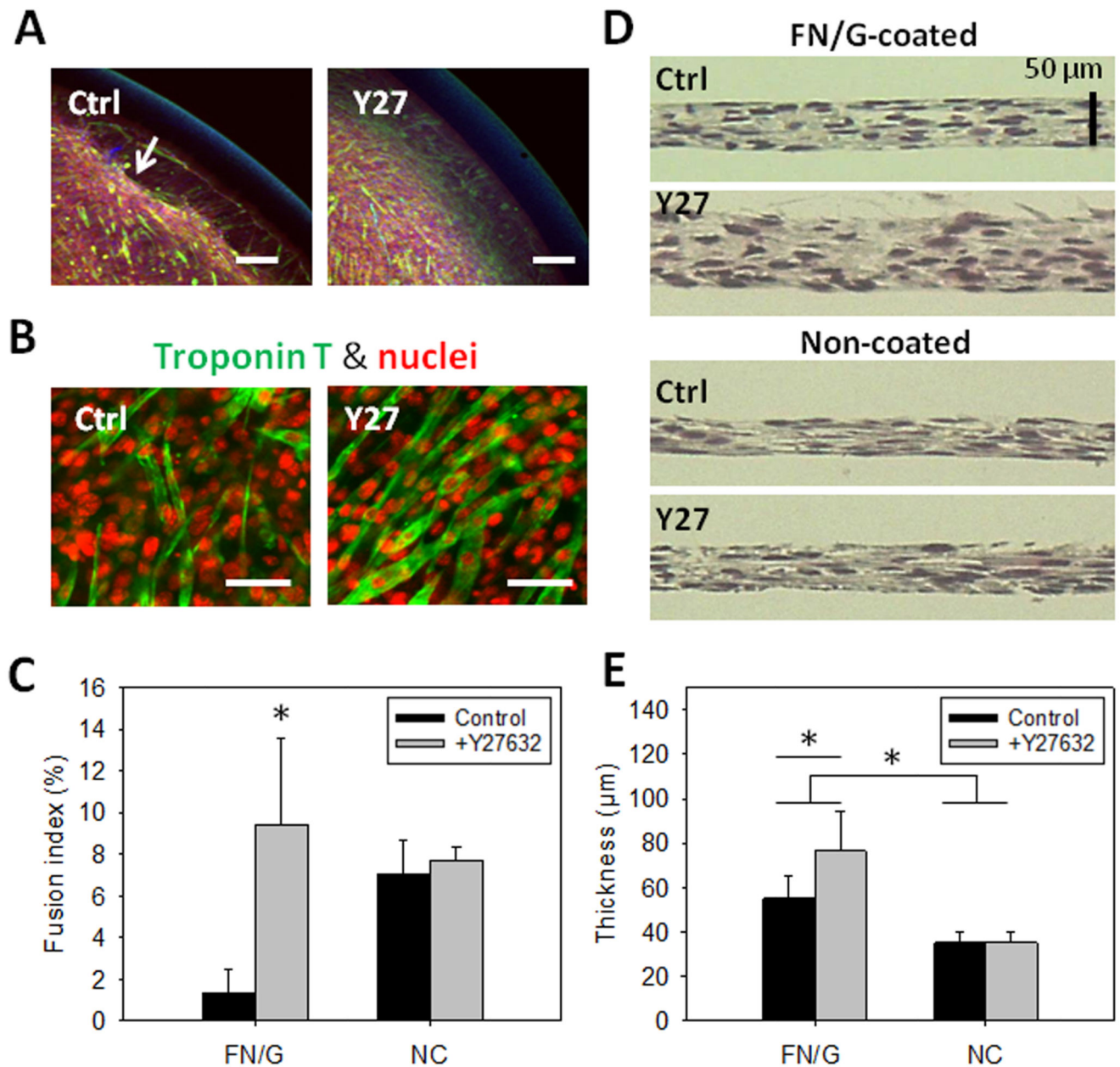
Fig 4. Rho-kinase inhibitor improves myogenic differentiation in FN/G-coated thick constructs.
(A) Effects of the Rho-kinase inhibitor Y27632 (Y27) on myogenic differentiation: observation of the insert periphery after 5 days of differentiation. Scale bar: 100 μm. (B) Confocal microscopy images of troponin T (green) and nuclei (red) staining of C2C12 cell constructs after 5 days in differentiation medium supplemented or not with 5 μM Y27632. Scale bar: 50 μm. (C) Fusion index of 10x FN/G-coated constructs at Day 5 of differentiation (n=2, *p<0.05 compared to all other conditions). (D) Phase contrast microscopy observations of hematoxylin-eosin stained cross-sections in Z of FN/G-coated and non-coated constructs after 4 days of culture in DM. Scale bar: 50 μm. (E)

Quantification of the thickness from histological cross-sections after 4 days of culture in DM (n=2, *p<0.05).

Table 1

Cell viability of FN/G-coated and non-coated constructs after 1 day in GM (n=3).

The cell viability has been evaluated by Trypan blue staining.

	Control	
	FN/G	NC
1x	95.7 ± 1.2 %	91.7 ± 1.5 %
5x	96.3 ± 2.5 %	91.0 ± 1.0 %
10x	97.3 ± 1.2 %	93.7 ± 1.2 %